Available online at www.sciencedirect.com
ScienceDirect
Journal of Photochemistry and Photobiology A: Chemistry 194 (2008) 136–142
Journal of Photochemistry and Photobiology A:Chemistry
www.elsevier.com/locate/jphotochem

# Lanthanide-centered luminescent hybrid microsphere-particles obtained by sol–gel method

Hai-Feng Lu [a], Bing Yan [a,b,*]

[a] *Department of Chemistry, Tongji University, Siping Road 1239, Shanghai 200092, China*
[b] *State Key Lab of Rare Earth Materials Chemistry and Applications, Peking University, Beijing 100871, China*

Received 26 April 2007; accepted 30 July 2007
Available online 6 August 2007

**Abstract**

Luminescent hybrid micro-particles have been prepared by traditional sol–gel method. The precursor derived from 2-amino pyridine exhibited a self-organization under the coordination to $RE^{3+}$ ($Eu^{3+}$, $Tb^{3+}$) evaluated by SEM (micrometric scale) and X-ray diffraction studies (nanometric scale). The adapting traditional routes used in this paper affected the shape of the materials and can be taken as a new method to control the hydrolysis-polycondensation process. Fourier transform infrared (FTIR), diffuse reflectance ultraviolet–visible spectra (DRUVS) and $^1$H NMR spectra were used to confirm the modifications. The material's phosphorescent spectra and luminescence spectra were recorded. The efficient intramolecular energy transfer process between carboxylic group and lanthanide ions took place within these molecular-based hybrids. The narrow-width green and red emissions were achieved for $Tb^{3+}$ and $Eu^{3+}$ ions, respectively.


*Keywords:* Chemical modification; Photoluminescence; Organic–inorganic hybrids; Microspheres; Sol–gel process

## 1. Introduction

Organic–inorganic hybrid materials have great potential for many applications due to the synergy between the properties of these two different building blocks. In general, the inorganic parts could offer the good mechanism properties and the organic parts are mainly taken as functional units. The choice of the organic group is very broad, permitting the promising applications in many fields including optics, electronics, membranes, protective coatings, sensors, etc. [1]. Lanthanide complexes are of particular interest for use in light-conversion devices in view of their long-lived excited-states characteristic and their especially efficient strong narrow-width emission band in the visible region [2]. In our group's previous research, the lanthanide ions ($Eu^{3+}$, $Tb^{3+}$, $Sm^{3+}$, $Dy^{3+}$) complexes with aromatic carboxylic acid [3,4], acylamide [5,6], pyridine [7] and their derivatives [8] have been investigated. The development of novel linkages for tethering organic compounds to inorganic solid supports is also an area of active investigation and there are four ways to synthesis lanthanide centered luminescent hybrid materials: amino-modification [3], hydroxyl-modification [4], carboxyl-modification [5,9], and sulfonic-modification [6].

Sol–gel method has been taken as the classical approach to prepare silica-based organic–inorganic hybrid materials due to the advantages such as low-temperature processing and easy shaping, higher sample homogeneity and purity [10]. Moreover, the location of the organic dyes can be priori tuned through dye–matrix interactions (covalent bonds, hydrogen bonds, ionic and van der Waals bonds) [11]. Even when all the silica materials obtained by sol–gel route are always amorphous systems, the possibility of self-organization in these hybrid materials has been demonstrated by using very specific organic precursors such as octadecyltrichlorosilane, chiral diureidocyclohexane or a bisurea-based precursor that exhibit a strong interaction by H-bonding [12–14]. Thus, the introduction of an organic group appeared like a factor favorable for the existence of an organization into these amorphous systems since the X-ray scattering exhibits diffraction signals, but never any Bragg peak [15]. Until now all the systems that have been studied correspond to linear spacers presenting rigid or semirigid or flexible geometries [16–18]. In all the cases investigated, only weak interactions

* Corresponding author at: Department of Chemistry, Tongji University, Siping Road 1239, Shanghai 200092, China.
*E-mail address:* byan@tongji.edu.cn (B. Yan).

1010-6030/$ – see front matter © 2007 Elsevier B.V. All rights reserved.
doi:10.1016/j.jphotochem.2007.07.034

between the organic moieties such as van der Waals, London, or π–π staking were able to induce an organization.

Thus, our specific investigations have concerned about the structure as well as the texture of the hybrid solids that how the coordination between the ions and the ligands in the sol–gel process can impact on the organization in those amorphous systems. We use 2-amino pyridine as the organic dyes. It can react with 3-(triethoxysilyl)-propyl isocyanate and the derived multifunctional organosilane precursor was afterward submitted to complex with $Eu^{3+}$/$Tb^{3+}$ ions and to a sol–gel process in order to obtain the anticipant hybrid materials. They are generally performed at room temperature where gelatine nanoparticles have to be stabilized by chemical cross-linking. As an alternative, we developed a oil-in-water nano-emulsion process involving the drying gelatine on a vacuum line, followed by the rapid condensation of silicates, leading to stable hybrid micro-particles. The structure of the deposited silica particles appears to depend on both organosilane concentrate and the coordination interactions.

## 2. Experimental

### 2.1. Chemicals and procedures

Starting materials were purchased from Aldrich or Fluka and were used as received except 3-aminopropyl trimethoxysilane which was provided by Lancaster Synthesis Ltd. and distilled before utilization. All normal organic solvents were purchased from China National Medicines Group and were distilled before utilization according to the literature procedures [19]. Terbium and europium nitrates were obtained from the corresponding oxides in dilute nitric acid.

The typical procedures for the preparation of hybrid precursor and hybrid material are described in Scheme 1(I). The hybrid precursor was prepared as follows: 0.56 g (6 mmol) 2-amino pyridine was first dissolved in 15 ml pyridine by stirring and then 1.48 g (6 mmol) 3-(triethoxysilyl)-propyl isocyanate was added to the solution by drops. The whole mixture was refluxing at 70 °C for 6 h. The solution was condensed to evaporate the solvent and then the residue was dried on a vacuum line. A yellow oil was obtained. $^1$H NMR ($CDC1_3$, 500 MHz) 0.73 (t, 2H, $H_3$), 1.22 (t, 9H, $H_1$) 1.75 (m, 2H, $H_4$), 3.40 (q, 2H, $H_5$), 3.83 (q, 6H, $H_2$), 6.84 (t, 1H, $H_{10}$), 6.89 (d, 1H, $H_8$), 7.55 (t, 1H, $H_9$), 8.14 (d, 1H, $H_{11}$), 9.12 (s, 1H, $H_6$), 9.44 (s, 1H, $H_7$).

The sol–gel derived hybrid was prepared as follows: 0.6 mmol hybrid precursor and 1.2 mmol tetraethoxysilane (TEOS) were dissolved in 5 ml ethanol with stirring. The mixture was agitated magnetically to achieve a single phase in a covered Teflon beaker for 4 h, and then 30 ml water was added under gentle magnetic stirring to form an initial o/w (oil-in-water) macro-emulsion for an hour. After that, it was dried on a vacuum line at 60 °C immediately. After aged until the onset of gelation which occurred, the gels were collected for the physical properties studies. It was named hybrid material I in this paper.

The sol–gel derived hybrid containing rare-earth ions was prepared as follows: 0.6 mmol sulfonamide precursor was dissolved in 5 ml ethanol with stirring. And 0.2 mmol

I

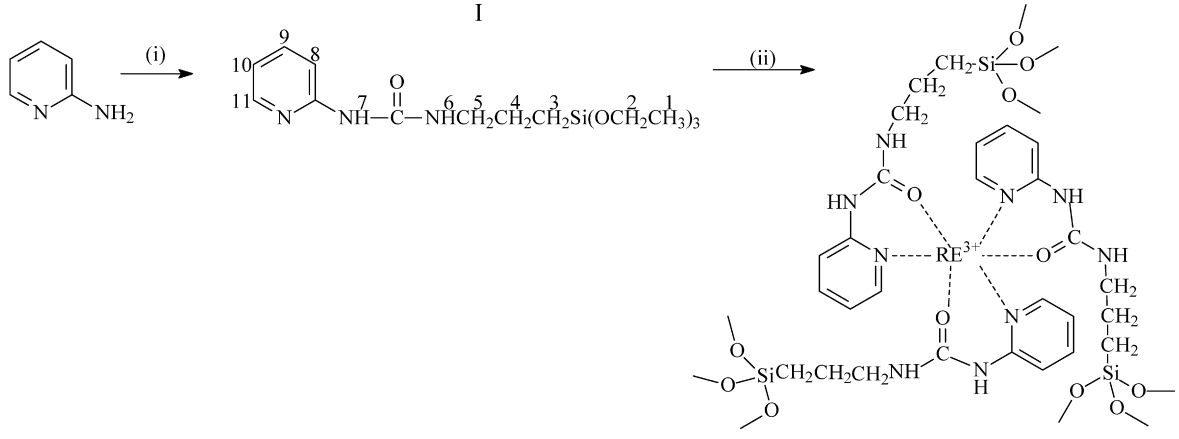


(i) 3-(triethoxysilyl)-propyl isocyanate, reflux, pyridine, 70¡æ, 6h;(ii) $RE(NO_3)_3$, TEOS, ethanol, rt, 4h

II

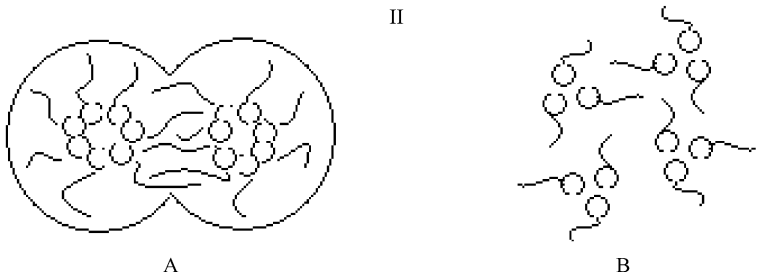

A B

Scheme 1. The typical procedures for the preparation of hybrid precursor and hybrid material (I); the hypothetic form mechanism of hybrid material II (A) and hybrid material II (B).

$RE(NO_3)_3{\cdot}6H_2O$ ($Tb(NO_3)_3{\cdot}6H_2O$ and $Eu(NO_3)_3{\cdot}6H_2O$, respectively) and 1.2 mmol tetraethoxysilane (TEOS) was added into the solution, respectively. The mixture was agitated magnetically to achieve a single phase in a covered Teflon beaker for 4 h, and then 30 ml water was added under gentle magnetic stirring to form an initial o/w (oil-in-water) macro-emulsion for an hour. After that, it was dried on a vacuum line at 60 °C immediately. After aged until the onset of gelation which occurred, the gels were collected for the physical properties studies. And they were named hybrid material II in this paper.

### 2.2. Measurements

Fourier transform infrared (FTIR) spectra were measured within the 4000–400 $cm^{-1}$ region on an (Nicolet model 5SXC) infrared spectrophotometer with the KBr pellet technique. $^1H$ NMR (Proton Nuclear Magnetic Resonance) spectra were recorded in $CDCl_3$ on a BRUKER AVANCE-500 spectrometer with tetramethylsilane (TMS) as inter reference. Diffuse reflectance ultraviolet–visible spectra (DRUVS) of hybrid materials were recorded with a BWSpec 3.24u_42 spectrophotometer. Phosphorescent spectra (chloroform solution) and luminescence (excitation and emission) spectra of these solid complexes were determined with a RF-5301 spectrophotometer whose excitation and emission slits were 5 and 3 nm, respectively. The X-ray diffraction (XRD) measurements were carried out on powdered samples via a "BRUKER D8" diffractometer (40 mA_40 kV) using monochromated Cu $K\alpha_1$ radiation ($\lambda = 1.54$ Å) over the $2\theta$ range of 10–70°. Scanning electronic microscope (SEM) images were obtained with a Philips XL-30.

## 3. Results

The FTIR spectra for 2-amino pyridine (a), the precursor (b), hybrid material I (c) and the hybrid material II (d) are shown in Fig. 1. The trident peaks at 3500–3200 $cm^{-1}$ in curve of 2-amino pyridine (a) is the unique vibration of $NH_2$ group and it turned into broad peak of $\nu$(N–H) at 3450–3300 $cm^{-1}$ in curve of precursor (b) [20]. Two adjacent sharp peaks at 2926 $cm^{-1}$ and 2886 $cm^{-1}$ in curve of precursors (b) are $\nu_{as}(CH_2)$ and $\nu_s(CH_2)$ of the long carbon chain in precursors. And $^1H$ NMR spectra relative to the precursors are in full agreement with the proposed structures. In the spectra of hybrid materials (I and II), the spectra are dominated by the $\nu$(Si–O–Si) absorption bands at 1120–1000 $cm^{-1}$. These indicated the formation of siloxane bonds [20]. The decrease of other peaks' intensities may be due to the containing of the organic groups by the silicate inorganic host which occurred in the hydrolysis and condensation process.

Coordination of lanthanide ions by the ligands is clearly shown by infrared spectroscopy. In spectrum of precursors (b), the $\nu$(C=O) vibrations is located at 1686 $cm^{-1}$. But in the spectrum of the hybrid material II (d), the $\nu$(C=O) vibrations is shifted to the 1596 $cm^{-1}$ while it keep constant in the spectrum of hybrid material I (c). The shift is a proof of the coordination

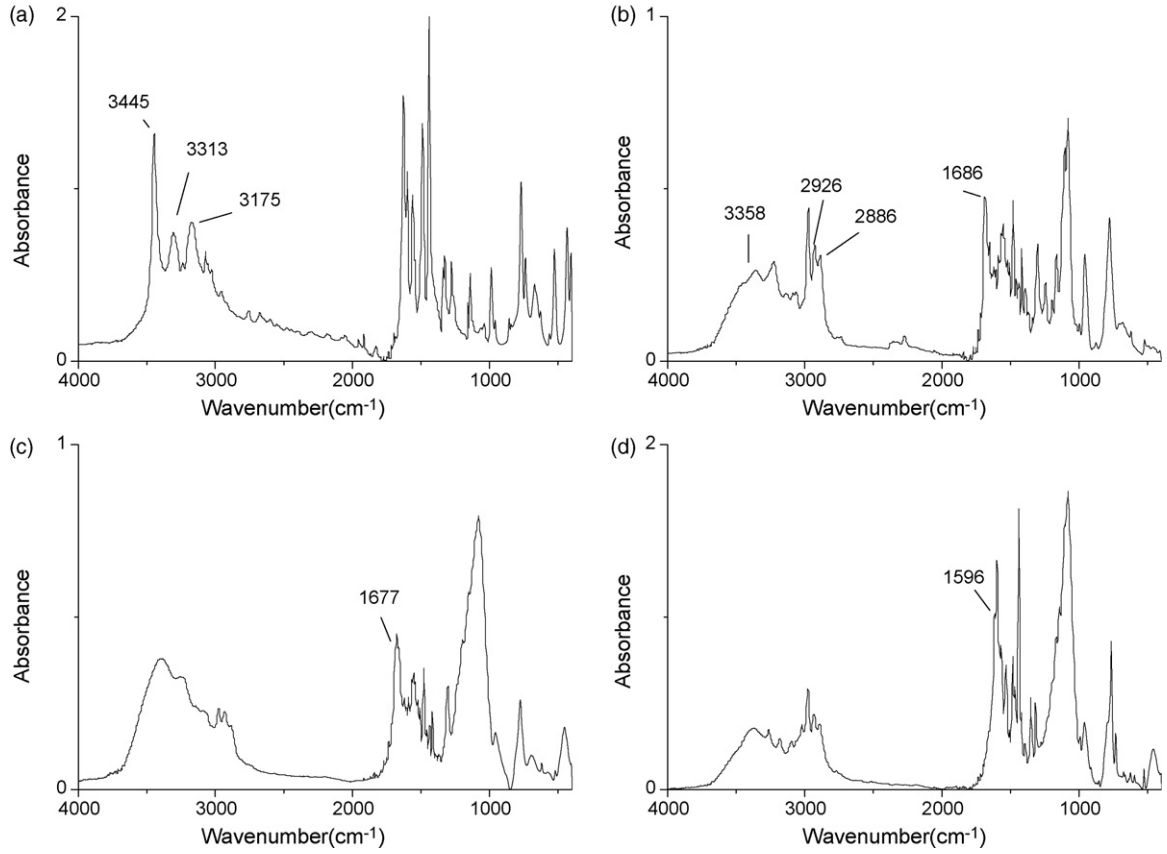


Fig. 1. Infrared spectra of 2-amino pyridine (a), the precursor (b), hybrid material I (c) and the hybrid material II (d).

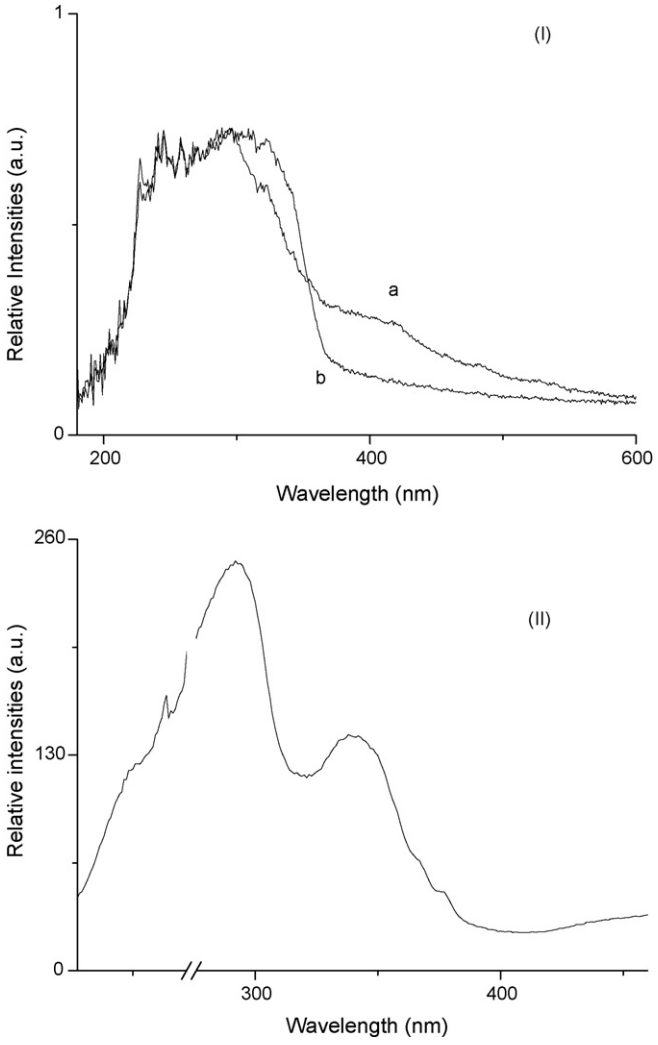


Fig. 2. Diffuse reflectance ultraviolet–visible spectra of hybrid material I (a) and hybrid material II (b) (I); the excitation spectra of the resulting hybrid material (II).

of the carbonyl group to the metallic ion with the oxygen atoms [9].

Fig. 2 shows the diffuse reflectance ultraviolet–visible spectra (DRUVS) of hybrid material I (a) and hybrid material II (b). In the spectra, the absorption peak around 260 nm corresponded to the $\pi \rightarrow \pi^*$ electronic transition of aromatic pyridine ring [20]. The red shift from 280 to 322 nm corresponds to the coordination of carbonyl oxygen to lanthanide ions. And the decrease around 400 nm between two kinds of hybrid materials (I and II) mainly caused by the lanthanide ions' f–f absorption [21].

## 4. Discussion

Carbonyl and heterocyclic nitrogen compounds are already well-known to be good chelating groups to sensitize luminescence of lanthanide ions [9]. The mechanism usually described as antenna effect: the ligand reinforce the energy absorbability and transfer it to the metal ion with high efficiency. Then the emission from the lanthanide ions' excited state will be observed [22].

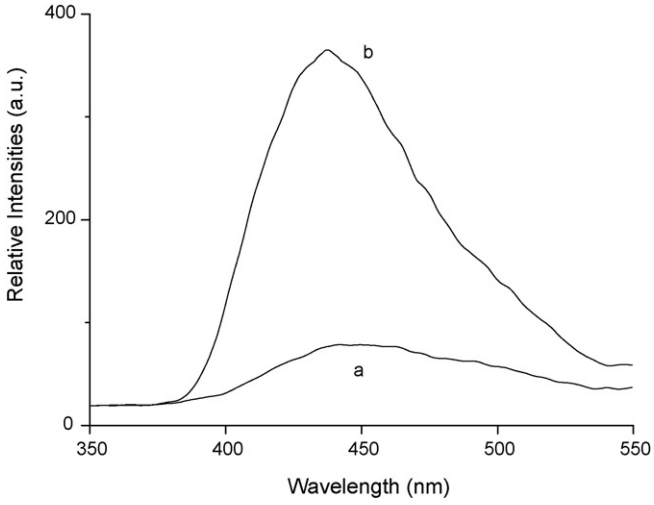


Fig. 3. Phosphorescence spectra of 2-amino pyridine (a) and the precursor (b).

The phosphorescence spectra of 2-amino pyridine (a) and the precursor (b) are recorded in Fig. 3. All of the curves exhibited a broad phosphorescence band which corresponds to the triplet state emission of them. An increase of peak intensity was observed between 2-amino pyridine and precursor because the modification of 2-amino pyridine brings carbonyl group into this system. The triplet state energy of carbonyl group is 2288 $cm^{-1}$ in the precursor. According to the energy transfer and intramolecular energy mechanism [23], it can be predicted that the triplet state energy of precursor is quite suitable for the luminescence of terbium ion (20,500 $cm^{-1}$) but poor for europium ion (17,250 $cm^{-1}$). Because the triplet state energy of ligand is higher than that of lanthanide ions, the energy could be transferred. But the span of the energy levels between the ligand and europium ion is too large which hampered the energy transfer.

Fig. 4 is the excitation spectra of the resulting hybrid materials, which are monitored at 545 nm under room temperature. The spectra exhibits two broad excitation bands centered at 290 nm and 340 nm in the UV range, respectively. The band around

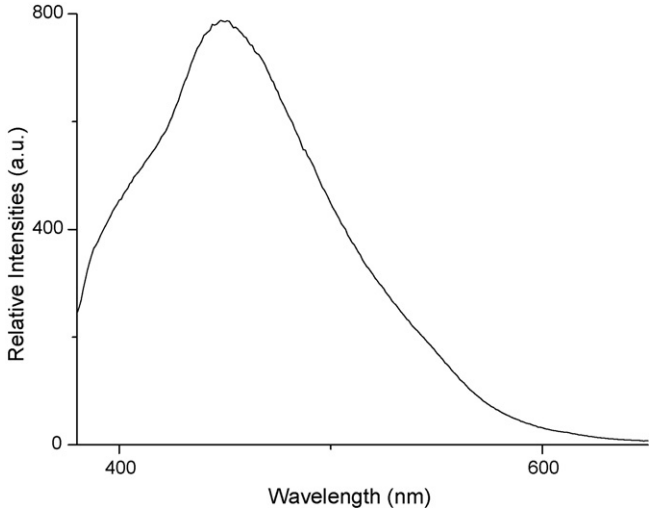


Fig. 4. The emission spectra of the hybrid material I.

290 nm corresponds to the singlet-to-singlet transitions of the organic groups in the materials and the band around 340 nm corresponds to ligand-to-metal charge transfer (LMCT) transition caused by interaction between the organic groups and the lanthanide ions [24,25]. No f–f transitions could be observed in the spectra (they are too weak).

The luminescence behaviors of all of the materials have been investigated at 298 K by direct excitation of the ligands (290 nm). Representative emission spectra are given in Figs. 4 and 5, respectively. It is a narrow-width red emission of europium hybrid materials. The narrow-width green emission is observed in the terbium hybrid materials.

Fig. 4 illustrates typical photoluminescence spectra of the hybrid material I. Because no lanthanide ions are doped in them, this kind of hybrid materials can only emit the luminescence of the organic group. The peak of the emission is located at 449 nm.

Fig. 5(I) illustrates typical photoluminescence spectra of the europium hybrid material. The maxima of these bands are at 590 and 613 nm which is associated with $^5D_0 \rightarrow {}^7F_1$ and $^5D_0 \rightarrow {}^7F_2$ transitions, respectively. The energy transfer from the carboxylic ligand to europium (III) is not perfect, as can be noticed to the residual ligand emission between 500 and 570 nm. It is not surprise because the poor energy level match has been described previously.

A prominent feature that may be noted in these spectra is the high intensity ratios of $I(^5D_0 \rightarrow {}^7F_2)/I(^5D_0 \rightarrow {}^7F_1)$. The intensity (the integration of the luminescent band) ratio of the $^5D_0 \rightarrow {}^7F_2$ transition to $^5D_0 \rightarrow {}^7F_1$ transition has been widely used as an indicator of $Eu^{3+}$ site symmetry [26]. When the interactions of the rare-earth complex with its local chemical environment are stronger, the complex becomes more nonsymmetrical and the intensity of the electric-dipolar transitions becomes more intense. As a result, $^5D_0 \rightarrow {}^7F_1$ transition (magnetic-dipolar transitions) decreased and $^5D_0 \rightarrow {}^7F_2$ transition (electric-dipolar transitions) increased. In this situation, the intensity ratios are approximately 2. This ratio is only possible when the europium ion does not occupy a site with inversion symmetry [24]. It is clear that the strong coordination interactions took place between the organic groups and lanthanide ions.

Fig. 5(II) illustrates typical photoluminescence spectra of the terbium hybrid material. Narrow-width emission bands with maxima at 487, 543, 580 and 619 nm are recorded. These bands are related to the transition from the triplet state energy level of $Tb^{3+}$ to the different single state levels and are attributed to the $^5D_4 \rightarrow {}^7F_6$, $^5D_4 \rightarrow {}^7F_5$, $^5D_4 \rightarrow {}^7F_4$ and $^5D_4 \rightarrow {}^7F_3$ transitions of $Tb^{3+}$ ions, respectively. The smoother baseline in the spectra suggests that energy transfer efficiency between the organic groups and $Tb^{3+}$ ions is higher than that between the organic groups and $Eu^{3+}$ ions.

The X-ray diffraction graphs of 2-amino pyridine (a), hybrid material I (b) and the hybrid material II (c) and hybrid material I doped with Terbium nitrates (d) are showed in Fig. 6. In the spectrum of 2-amino pyridine (a), there are characteristic X-radiation peaks of 2-amino pyridine crystals. But the diffractogram of the hybrid materials reveals that all of the hybrid materials with $10^\circ \leq n \leq 70^\circ$ are totally amorphous. To hybrid material I (b), there is only a broad peak centered 21.56° while there are two broad peaks centered around 10° and 23.88° in

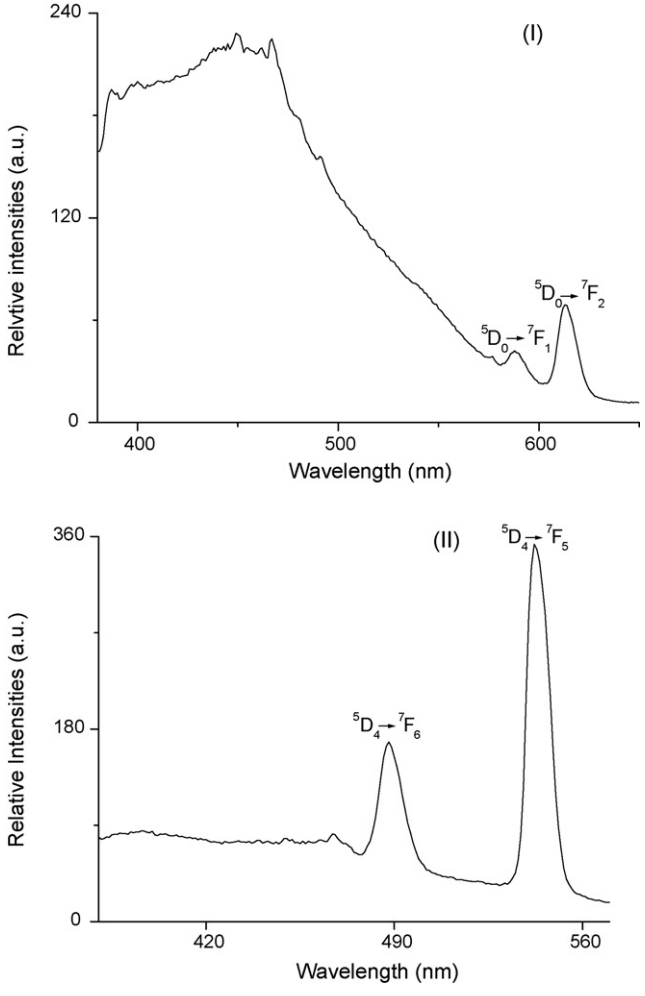


Fig. 5. The emission spectra of the europium hybrid material (I) and the emission spectra of the terbium hybrid material (II).

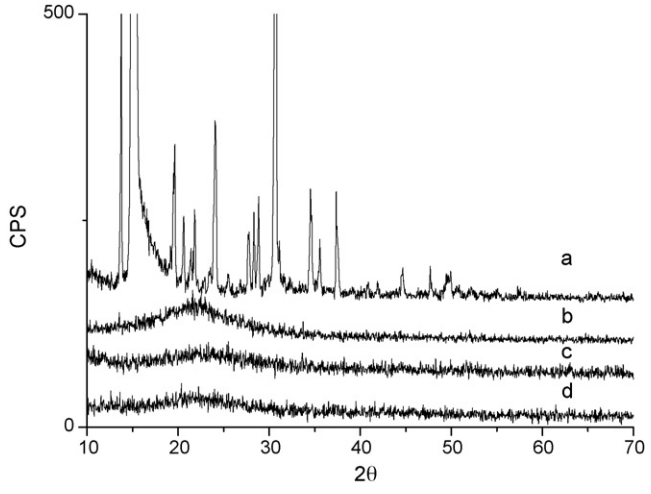


Fig. 6. The X-ray diffraction graphs of 2-amino pyridine (a), hybrid material I (b) and the hybrid material II (c) and hybrid material I doped with terbium nitrates (d).

the hybrid material II (c). To exclude the impact of lanthanide nitrates, hybrid material I doped with Terbium nitrates according to the ratio of previous experiment description are prepared and its XRD spectrum (d) is measured. From the spectra, it is clear that neither free europium/terbium nitrates salt, pure crystalline thiosalicylic acid nor crystalline lanthanide complexes occurs throughout the range of those materials. The absence of any crystalline regions in these samples correlates well with the presence of organic chains in the host inorganic framework.

The scanning electron micrographs (SEM) of these hybrid materials demonstrate that micro-particle materials were obtained (see Fig. 7). Most of the hybrid material I are sphere (top graph in Fig. 7). These are mostly owing to the adapting sol–gel treatment. In the sol process, the o/w macro-emulsion is decisive and responsibility for the materials' final texture. The isolated sphere is easy to understand because the weak interactions between the organic moieties such as van der Waals, London, or π–π staking were able to induce an organization [16–18]. For the disphere particle, it may be supposed that pervasions take place between two spheres (see A in Scheme 1(II)). The texture of hybrid material II seems to be largely different with hybrid material I while they were prepared by same process (right graph in Fig. 7). A hypothesis is proposed in Scheme 1(II—B). Because of the coordination between organic groups and lanthanide ions, the configuration of the organosilane is mixed up and it is difficult to form an organization under the weak interactions such as π–π staking.

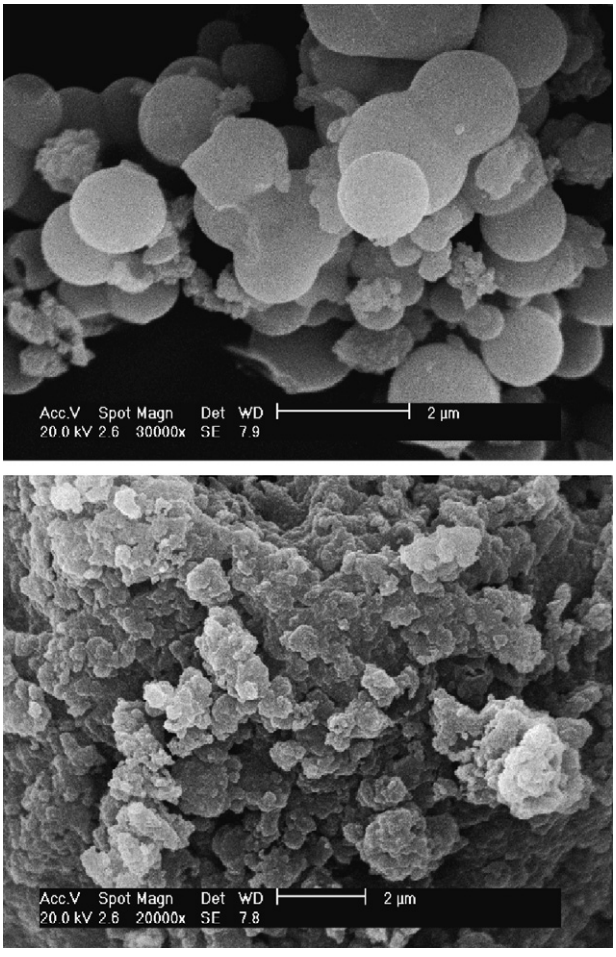


Fig. 7. The scanning electron micrographs of the hybrid material.

## 5. Conclusions

In this work, a new route to gelatine and hybrid microparticles was described, based on an o/w process and organosilane polycondensation. This result validates our previous assumption that the coordination between the ions and the ligands in the sol–gel process can impact on the organization in those amorphous systems. Although all the hybrid materials are amorphous, the organization does exist and could be adjusted. When compared to the previously reported silica hybrid materials [1–9], this system presents a number of advantages: (i) the hybrid particles exhibit a micrometric structure, and not a continuous hybrid network, so that they are convenient to use and need not to be ground; (ii) the synthesis does not involve any high-temperature process and the time needed is shortened. As far as particle internalization is concerned, experiments suggest that the coordination impacts largely on the texture of the final material. However, efforts are still needed to control the particle size dispersion, a key parameter for industry usage. In the case of emulsion-based processes, the possibility to obtained monodisperse materials will be a promising candidate to prepare many new multifunctional hybrid materials.

## Acknowledgement

This work was supported by the National Natural Science Foundation of China (20671072).

## References

[1] C. Sanchez, G.J. de, A.A. Sloer-Illia, F. Ribot, T. Lalot, C.R. Mayer, V. Cabuil, Chem. Mater. 13 (2001) 3061.
[2] L.R. Matthews, E.T. Knobbe, Chem. Mater. 5 (1993) 1697.
[3] Q.M. Wang, B. Yan, J. Mater. Chem. 14 (2004) 2450.
[4] L.M. Zhao, B. Yan, Appl. Organomet. Chem. 19 (2005) 1060.
[5] Q.M. Wang, B. Yan, Inorg. Chem. Commun. 7 (2004) 747.
[6] H.F. Lu, B. Yan, J. Non-Cryst. Solids 352 (2006) 5331.
[7] Q.M. Wang, B. Yan, J. Photochem. Photobiol. A Chem. 178 (2006) 70.
[8] Q.M. Wang, B. Yan, Inorg. Chem. Commun. 7 (2004) 1124.
[9] A.C. Franville, D. Zambon, R. Mahiou, Chem. Mater. 12 (2000) 428.
[10] U. Schubert, N. Husing, A. Lorenz, Chem. Mater. 7 (1995) 2010.
[11] C. Sanchez, B. Lebeau, F. Chaput, J.P. Boilot, Adv. Mater. 15 (2003) 1969.
[12] A. Shimojima, Y. Sugahara, T. Ohsuna, O. Terasakl, Nature 416 (2002) 304.
[13] J.J.E. Moreau, L. Vellutim, M.W.C. Man, C. Bied, J. Am. Chem. Soc. 123 (2001) 1509.
[14] J.J.E. Moreau, L. Vellutim, M.W.C. Man, C. Bied, J.L. Bantignles, P. Dieudonne, J.L. Sauvajol, J. Am. Chem. Soc. 123 (2001) 7957.
[15] G. Cerveau, R.J.P. Corriu, E. Framery, F. Lerouge, Chem. Mater. 16 (2004) 3794.
[16] B. Boury, F. Ben, R.J.P. Corriu, P. Delord, M. Nobili, Chem. Mater. 14 (2002) 730.
[17] M.C. Goncalves, V.deZ. Bermudez, R.A. Sa Ferreira, L.D. Carlos, D. Ostrovskii, J. Rocha, Chem. Mater. 16 (2004) 2530.
[18] B. Boury, R.J.P. Corriu, Chem. Commun. 795 (2002).
[19] D.D. Perrin, W.L.F. Armarego, D.R. Perrin (Eds.), Purification of Laboratory Chemicals, Pergamon Press, Oxford, 1980.

[20] E. Pretsch, P. Buhlmann, C. Affolter (Eds.), Structure Determination of Organic Compounds, second printing, Springer, Berlin, 2003.
[21] G. Blass, B.C. Grabmaier (Eds.), Luminescent Materials, Springer, Berlin, 1994.
[22] G. Crosby, R.E. Whan, R. Alire, J. Chem. Phys. 34 (1961) 743;
J. Genzer, J. Groenewold, Soft Matter 2 (2006) 310.
[23] S. Sato, M. Wada, Bull. Chem. Soc. Jpn. 43 (1970) 2403.
[24] K. Binnemans, P. Lenaerts, K. Driesen, C. Gorller-Walrand, J. Mater. Chem. 14 (2004) 191.
[25] O.L. Malta, H.F. Brito, J.F.S. Menezes, Luminescence 75 (1997) 255.
[26] Z. Wang, J. Wang, H.J. Zhang, Mater. Chem. Phys. 87 (2004) 44.